POLITECNICO DI TORINO
Repository ISTITUZIONALE

Integrated Health Monitoring for Robust Actuation System of UAV Primary Flight Controls

(Article begins on next page)

26 April 2024

International Journal
of
Mechanics and Control

Editor: Andrea Manuello Bertetto
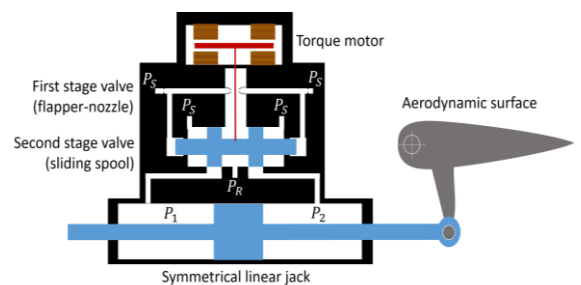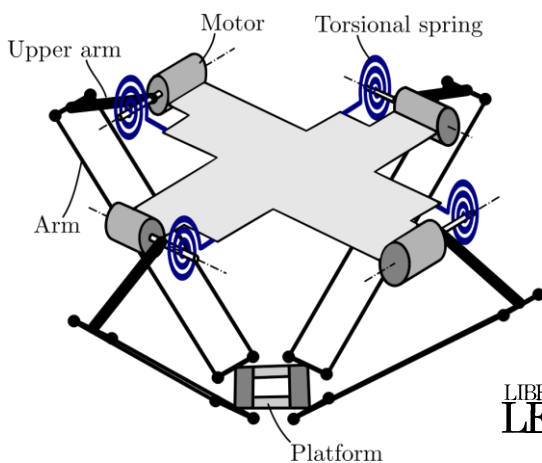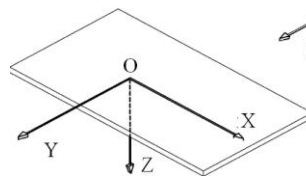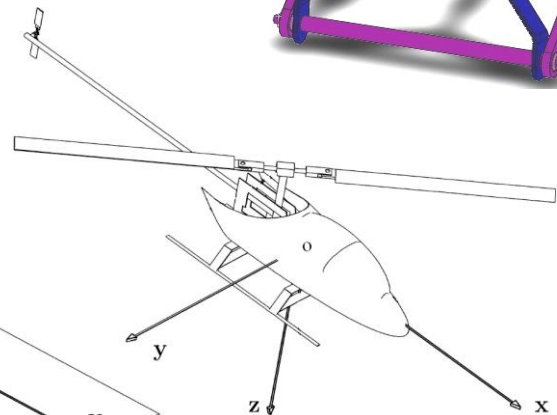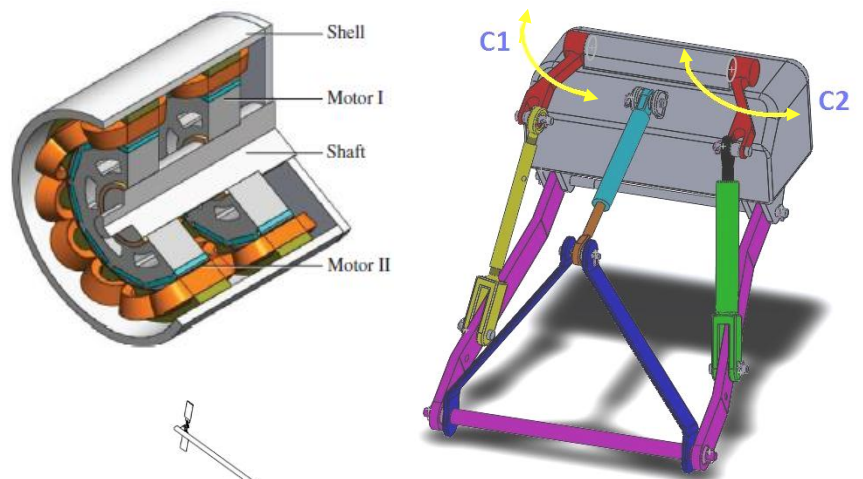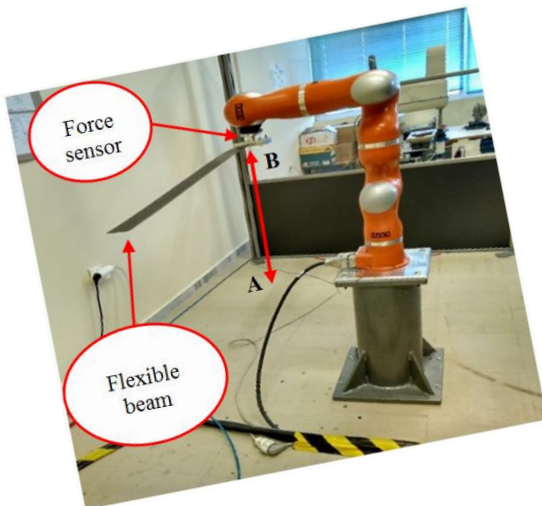
International Journal of Mechanics and Control

Associate Editors

Published by Levrotto&Bella – Torino – Italy E.C.

International Journal of Mechanics and Control

The Journal is addressed to scientists and engineers who work in the fields of mechanics (mechanics, machines, systems, control, structures). It is edited in Turin (Northern Italy) by Levrotto&Bella Co., with an international board of editors. It will have not advertising.

Turin has a great and long tradition in mechanics and automation of mechanical systems. The journal would will to satisfy the needs of young research workers of having their work published on a qualified paper in a short time, and of the public need to read the results of researches as fast as possible.

Interested parties will be University Departments, Private or Public Research Centres, Innovative Industries.

Aims and scope

The *International Journal of Mechanics and Control* publishes as rapidly as possible manuscripts of high standards. It aims at providing a fast means of exchange of ideas among workers in Mechanics, at offering an effective method of bringing new results quickly to the public and at establishing an informal vehicle for the discussion of ideas that may still in the formative stages.

Language: English

International Journal of Mechanics and Control will publish both scientific and applied contributions. The scope of the journal includes theoretical and computational methods, their applications and experimental procedures used to validate the theoretical foundations. The research reported in the journal will address the issues of new formulations, solution, algorithms, computational efficiency, analytical and computational kinematics synthesis, system dynamics, structures, flexibility effects, control, optimisation, real-time simulation, reliability and durability. Fields such as vehicle dynamics, aerospace technology, robotics and mechatronics, machine dynamics, crashworthiness, biomechanics, computer graphics, or system identification are also covered by the journal.

International Journal of Mechanics and Control

Scientific Board

Published by Levrotto&Bella – Torino – Italy E.C.

INTEGRATED HEALTH MONITORING FOR ROBUST ACTUATION SYSTEM OF UAV PRIMARY FLIGHT CONTROLS

Andrea De Martin*   Giovanni Jacazio*   Massimo Sorli*

* Politecnico di Torino - Department of Mechanical and Aerospace Engineering

ABSTRACT

The research activity described in this paper is aimed at developing a high integrity mechatronic system for UAVs primary flight controls able to ensure the necessary flight safety and to enhance the system availability by implementing appropriate Prognostics and Health Management functions. In this system a flight control surface is driven by two parallel rollerscrew driven by brushless motors equipped with gearhead and clutches; the motors electric drives are controlled by dual redundant electronic units performing closed loop position control. Provisions are taken in the motor drives to provide damping in the event of simultaneous failure of both actuators. The electronic units perform control, diagnosis and prognosis of the actuation system and mutually exchange data via a cross channel data link. System health monitoring and prognosis is performed by dedicated algorithms based on a combination between particle filtering, Artificial Neural Networks and data driven techniques processing the control and feedback signals during flight and dedicated preflight checks. A smart mechatronic system is obtained providing high integrity control of an aerodynamic surface with dual mechanical link, dual power source and quadruplex control.

Keywords: EMA, flight control system, PHM, prognostics, Health Monitoring

1 UAV PRIMARY FLIGHT CONTROLS ACTUATORS REQUIREMENTS

Pursuing an enhanced reliability is an essential need to improve UAVs' mission availability. This is a critical issue for UAVs, since system redundancies are often omitted to reduce cost and weight, taking shortcuts that would be unacceptable in manned aircraft. As with reliability, survivability is often traded for lower acquisition costs since an aircraft loss is a more acceptable risk when no aircrew is involved. A less than optimal survivability can be theoretically accepted for UAVs performing highly dangerous missions, but it thwarts the willingness of using them if UAVs repeatedly fail to accomplish their mission objectives. High survivability is therefore necessary to ensure that UAVs are mission effective. Flight Control Systems (FCSs) have historically been the single largest contributor to UAVs incidents [1-4].

Contact author: Andrea De Martin[1]

[1] Corso Duca degli Abruzzi 24, 10129, Torino, Italy.
  E-mail: andrea.demartin@polito.it

As such, reliability improvements in this area would critically contribute to reduce the mishap rate, hence resulting in savings of new UAVs acquisition costs and in improved UAVs effectiveness in accomplishing their missions. Today technologies applicable to UAVs flight control systems offer options for improving their reliability and survivability, and for reducing their life cycle costs resulting from decreased line maintenance.

Electromechanical actuation for primary flight controls has since long been seen as a technology able to improve the flight control system Mid Time Between Failures (MBTF) with respect to the hydraulic, as often observed in literature [5-12]; the most frequent cause of failure in hydraulic flight controls is represented by leakages occurrence in one or more of the hydraulic components, whereas the causes might be extremely different (worn out or extruded seals, misalignments, pipes issues etc.). Moreover, electromechanical actuators sensibly improve the maintainability of the FCS: there is no need of periodical replacement of the hydraulic fluid and of the filters, while the actuators replacement is made easier by the simpler access to power and control wiring. A second promising technology is the implementation of advanced diagnostics and failure prognosis to reduce the aircraft downtime by

offering the ground crew with enhanced capability of identifying the occurrence of faults in the FCS before their evolution into failures and, wherever possible, to track and forecast their growth to predict the Remaining Useful Life (RUL) up to the failure occurrence. This would allow for more accurate implementation of Condition Based Maintenance, ensuring a rapid turnaround and a maximum sortie rate for the UAVs. Moreover, this information would provide a better understanding of the UAVs conditions to the mission planning, improving their capability to respond with meaningful tactical decision in case a fault is recognized during a mission. The challenge associated to the introduction of these technologies is to devise solutions such that reliability, maintainability and availability gains exceed the nonrecurring investments and do not lead to unacceptable weight increases that would reduce the efficiency of the air vehicle. However, the potential advantages obtainable from electromechanical actuation and advanced diagnostics and prognostics for primary flight control actuators make a strong case for developing solutions incorporating these technologies. The architecture of a UAV flight control system depends on the intended use of UAV. According to Lucas and Seward [13] we can identify three different types of UAV flight control actuators, function of the UAV mission. Type I actuator has full electrical and mechanical redundancy and is suitable for UAVs approved for use in US National Airspace system. Type II actuator has only electrical redundancy, is used for different types of military operations, but is not approved for flight in civil airspace. Type III actuator is for low-cost UAVs used for less critical missions, it does not exhibit redundancies and is a step up from an industrial actuator. The research activity presented in this paper was focused on type I actuators. The flight control actuator that was eventually defined is a smart electromechanical actuator provided with enough intelligence to perform actuator control, monitoring, diagnostics and prognosis.

The definition of the flight control actuator was made with reference to the primary flight control surface of a large UAV with the following main design characteristics:

• Two independent 270 Vdc and four independent 28 Vdc electrical power supplies are available
• The flight control surface must be provided with two independent mechanical links
• Actuator stall load is 50000 N
• Actuator travel is 70 mm
• No load actuation rate is 70 mm/s
• System inertia reflected is 150 kg
• Required frequency response is $< \pm 1$ dB and $< 60°$ up to 5 Hz.

2 CRITICAL ISSUES OF ELECTROMECHANICAL FLIGHT CONTROL ACTUATORS

The main drive for using electromechanical actuators for the primary flight controls in place of the traditional hydraulic solution applied on manned aircrafts is in the several advantages resulting from the removal of the aircraft hydraulic system with its associated weight, maintainability and reliability issues. However, a critical issue with electromechanical actuators is the possibility of a seizure of any of their internal mechanical components, that would prevent the operation of the associated flight control surface even in the case of architectures provided with multiple actuators. Although the probability of such event is low, being in the order of 2 to 5 10^{-8} per flight hour, it is generally considered too large for the primary flight control actuator of manned aircrafts, which require a probability of jamming lower than 10^{-9} per flight hour. A possible architectural solution to cope with the possible jamming of an electromechanical actuator is to provide UAVs with multiple redundant flight control surfaces, such to ensure enough controllability of the aircraft in the event of hardover failure of an actuator in the fully deployed position of the flight control surface. This solution comes however with several disadvantages, since multiplying the number of movable aerodynamic surfaces makes the entire flight control system much more complex and heavier, particularly if each flight control surface must be driven by two actuators to prevent free floating in case of an actuator fracture. In order to address the issue of a possible actuator seizure many research and development activities have been performed and are under way to identify ways of making an electromechanical actuator jam-free or jam-tolerant, since this would allow more flexibility in defining the overall architecture of the flight control system. Although interesting and ingenious design solutions have been proposed, they all have resulted in complex mechanical designs that on one hand allow the actuator to operate after a jam of an internal component, but on the other hand bring about increased weight, volume and cost, and a reliability reduction due to the much larger number of parts. A second critical issue with electromechanical actuators is the heat dissipation. It often happens that while the aircraft is cruising or loitering, the flight control surface is stationary while being subjected to a load; in this condition an electrical current is drawn by the electric motor to generate the torque, and hence the actuator force, necessary to balance the external load. This generates heat in the motor windings and in the motor power bridge that must be transferred outside the actuator to limit the temperature to a safe value. A second heat source is given by the regeneration energy that originates when the actuator drives the flight control surface under aiding load conditions. The energy flowing back into the actuator must be dissipated as heat in a suitable electric circuitry within the motor drive, although studies are under way to store it in a supercapacitor added to the motor drive. A third possible source of heat generation is associated to a force fighting between two actuators simultaneously controlling the flight control surface. A traditional solution taken to avoid this condition is to control the two actuators in an active / standby mode. This is a simple control strategy, but it entails two main drawbacks: it requires more actuation

power because the active actuator must provide in normal conditions the force necessary to drive the standby actuator in addition to the flight control surface, and it leads to much larger transient disturbances following an actuator failure, because the flight control surface is uncontrolled for the time interval from the failure onset until the failure is recognized and the standby actuator is switched to the active mode. The issue of electromechanical actuator seizure can be overcome in two ways: either designing the actuator such to be jam tolerant, or to identify ways to early recognize actuator degradations that could lead to a seizure, thereby creating an alert before the seizure occurs. The issue of heat generation can be mitigated by using an active / active control strategy for the two actuators connected to the same flight control surface and by simultaneously implementing appropriate equalization techniques to obtain a fairly equal load share between the two actuators. By doing so, the aerodynamic load on the flight control surface is balanced by the forces developed by the two actuators, whose electric motors draw a current that is about half of that required for a single motor operation. Since the heat dissipation in the motor windings is proportional to the square of the current, an active / active control leads to a great reduction of the heat generation and to an associated improvement of the overall system efficiency. This is of course not true any longer in case of failure of one of the two actuators, but operation at higher than normal temperature of the electric motor and of its drive can be accepted for limited time without impairing their function or their reliability. Active / active control can thus offer several advantages but requires the implementation of suitable equalization algorithms and the continuous exchange of information between the two actuators driving the same aerodynamic surface.

3 PAST WORK ON JAM TOLERANT ELECTROMECHANICAL ACTUATORS

Several studies focused on possible configurations of jam-tolerant electromechanical actuators, some of which have been patented. An electromechanical actuator typically consists of an electric motor, a gear reducer and a ballscrew or rollescrew actuator converting rotary motion into linear. The solutions proposed for making the actuator jam tolerant can be broadly grouped in three different categories. The first category consists of actuators which design addresses only the possible jam occurrence located in the screw; this is for instance the case of the V-22 pylon conversion actuator [2]. This is however only a partial solution, because the ballscrew is only one of the several mechanical parts of the actuator that could possibly jam. Data on jammed mechanical actuators coming from the field seem to indicate that the gearing between the motor and the ballscrew is the actuator part most likely subjected to a seizure. Making a screw jam tolerant is normally obtained by using a telescopic ballscrew, consisting of primary and secondary screw: if the primary one jams, then the

secondary allows the motion transmission from input to output. However, if the full nominal travel capability must be retained after a jam, each of the two screws must be designed for a total travel equal to two times the nominal one, which makes the actuator much longer, an hence much heavier, than a conventional actuator. A second group of jam tolerant actuators design sees those solutions allowing the actuator to operate following the seizure of any of its internal parts. These solutions are based on two alternative ideas:

- designing an actuator with a dual parallel drive path, with the two paths ends speed summed on a balance beam
- providing the actuator with the possibility of moving its whole housing with respect to the airframe in case of actuator jam.

A design concept of a jam tolerant actuator following the first solution (two parallel drive paths and balance beam) is reported in Fig. 1. The output rod is connected to the flight control surface and the housing is connected to the airframe. The outputs of the two ballscrews are speed summed on a balance beam; under normal conditions the clutch is engaged and the two ballscrews are driven at the same speed by the electric motor. In case of jam of any part of the actuator, electric power is removed and the clutch is disengaged; the two drive paths are hence free to move independently: whichever of the two drive paths is jammed remains stationary, while the other drive path can be driven by the other actuator connected to the same flight control surface. A design concept of a jam tolerant actuator with movable housing is instead shown in Fig. 2. The primary ballscrew is connected to flight control surface while the secondary ballscrew is connected to airframe.
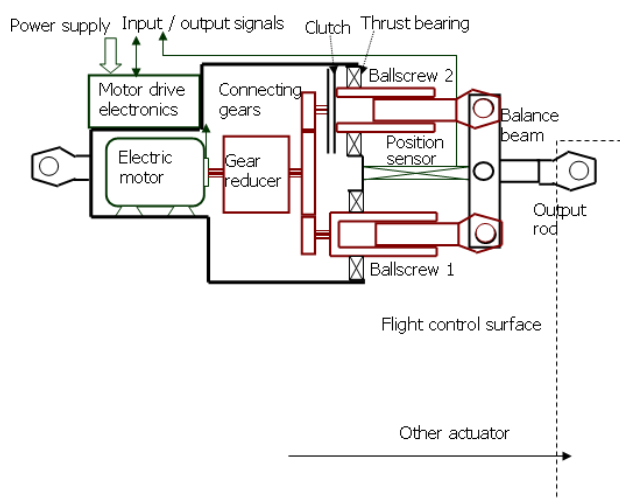

Figure 1: Design concept of a jam tolerant actuator with parallel drive paths and balance beam

Under normal operating conditions the primary electric motor is active while the secondary electric motor is braked; hence the primary ballscrew moves while secondary ballscrew is stationary.

In case of jam of the primary load path, the primary motor brake is activated and the motor drive electronics switches control from primary to secondary electric motor; the primary ballscrew then remains fixed in the last attained position while secondary ballscrew operates causing a movement of the entire actuator housing with respect to the airframe. These actuators concepts provide the jam tolerant capability, but at the expense of a significant increase in the design complexity. This translates into an increased number of parts with respect to a conventional actuator, significantly higher volume and weight.

Moreover, each individual ballscrew stroke must be sized at least the double of the nominal actuator travel to ensure the complete range of movements even in case of jamming in one of the power lines. Finally, we highlight a few design schemes featuring a disconnection device that mechanically separates the actuator output rod from the flight control surface. Although this concept seems in principle the most viable, the implementation of this solution in a practical design proved to be very difficult, and concerns on its reliability stymied the efforts in this direction.
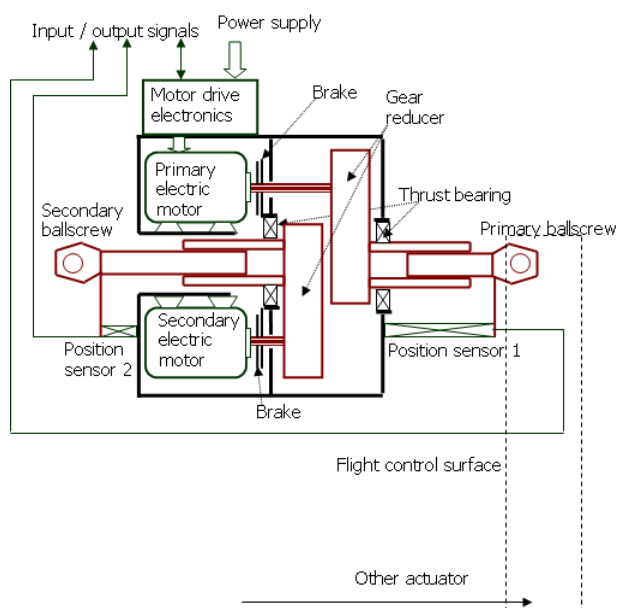
Figure 2: Design concept of a jam tolerant actuator with dual power source and movable housing

4 NEW APPROACH: AN INTEGRATED MECHATRONIC ACTUATION SYSTEM

A completely different approach for a robust electromechanical servo-actuator suitable for application to the primary flight controls of a UAV is hereby presented. The foundational idea is not to design an electromechanical actuator to be absolutely jam-tolerant, but to make the in-flight jam of the actuator a remote event, with a probability of occurrence comparable to that of the hydraulic actuators

technology. The three design criteria followed to achieve this results are,

- To enhance the actuator reliability by reducing the number components as much as possible while remaining consistent with a sound design;

- To ensure the mechanical disconnection of the parts of the actuator with largest probability of seizure, and implement this function with a simple design without the need of allowing dual travel to cope with the seizure

- To design and implement appropriate health monitoring functions to detect any anomalous behavior, and define robust prognostics routines to forecast failure occurrence

The system is made of two smart electromechanical actuator controlling the position of a UAV flight control surface; the combination of the two smart actuators, mutually exchanging information, defines a mechatronic system able to reach the safety requirements. The system scheme is represented in Fig. 3. It is made of two rollerscrew actuators connected in parallel to a flight control surface as done with conventional electrohydraulic servocontrols. The rollerscrews are driven by Brushless-DC motors with a gearhead and a clutch; each electrical drive is controlled by a dual-redundant remote electronic unit which close the position control loop in function of the position commands received via serial lines from the aircraft flight control computer. Provisions are taken in the motor drives to accept the regeneration of energy under aiding load conditions and to provide surface damping in the event of a simultaneous failure of the two actuators. The remote electronic units perform control, diagnosis and prognosis of the actuation system and mutually exchange data via a cross channel data link. System prognosis is made possible by the combination of the actuator design with the processing by means of dedicated algorithms of the control and feedback signals obtained in flight and during preflight checks. The two electromechanical actuators, with their motor drives and remote electronic units behave as a smart mechatronic system providing high integrity control of an aerodynamic surface with dual mechanical link, dual power source and dual control, similarly at what is done with fly-by-wire hydraulic flight control systems of manned aircraft. The system uses a rollerscrew rather than the more commonly adopted ballscrews to transform the motion from rotary into linear. Rollerscrews have a slightly lower efficiency than ballscrews but offers two advantages: they are less prone to jamming and can be manufactured with a lower lead than for ballscrews with the same load capacity. This second characteristic entails a higher angular speed of the screw input for the same linear velocity of the screw output; as a result, lower speed reduction is required from the electric motor to the screw input and a simpler gear reducer can be used. In general, a rollerscrew can have a lead about 2.5 times smaller than that of a ballscrew carrying the same load, which implies one less stage in the

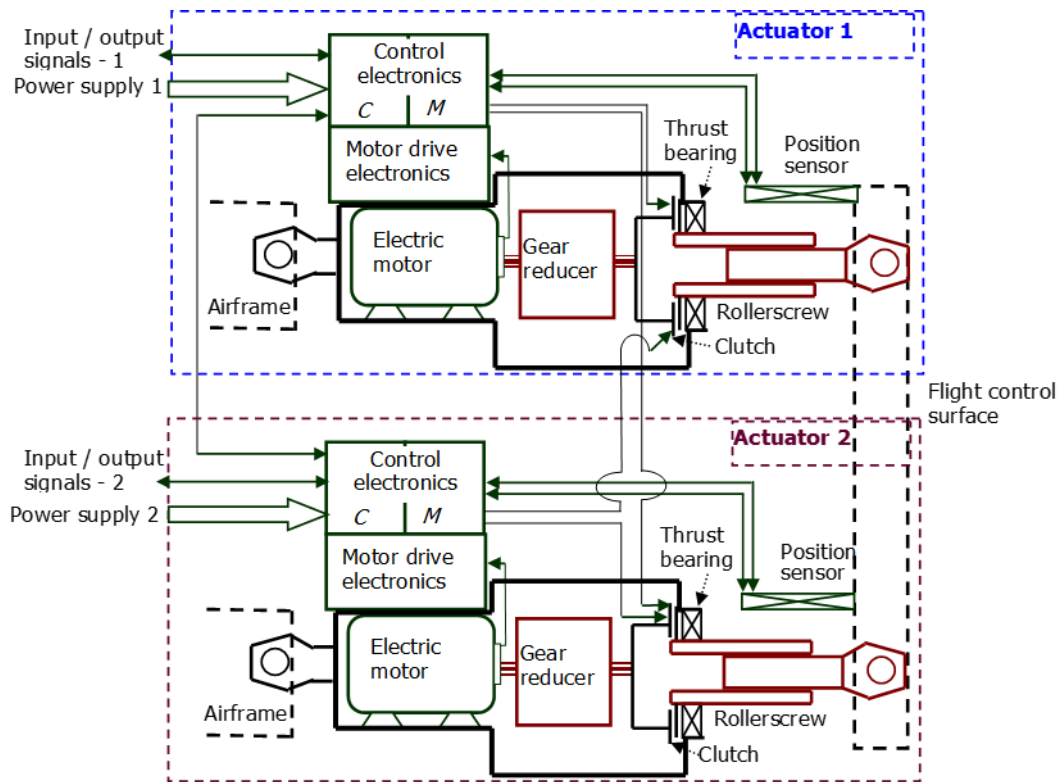Figure 3: Diagram of the mechatronic system for position control of a primary flight control surface

gear reducer. An actuator required to operate against a load of 35000 N at a speed of 40 mm/s (1.4 kW of output power) can be designed with a 5 mm lead ballscrew rotating at 480 rpm, or with a 2 mm rollerscrew rotating at 1200 rpm. For this power range an electric motor running around 5000 rpm is a good compromise between efficiency and weight, which implies a dual reduction stage for the case of a ballscrew actuator, but a single reduction stage for a rollerscrew actuator. Hence, the end result is an increased actuator reliability. In the scheme, rollerscrews are shown with rotating nut and translating screw, but they can as well be made of a rotating screw and a translating nut. The rotating part of the rollerscrew is connected to the gear reducer output by means of a clutch that is spring engaged and can be disengaged by electrical signals coming from either of the two actuators electronic control units. The clutch can be directly mounted on the rollerscrew nut because its large angular speed entails low torque and hence low weight and volume of the clutch. A single-stage gear reducer provides speed reduction from the electric motor to the clutch. If the system is operating normally, no electrical signal is sent from the actuators control electronics to the clutches of the two actuators, which are thus engaged and transmit the mechanical power. If any failure of actuator 1 occurs, including a power loss or a failure of its own control electronics, the failure is detected by the monitoring system and the control electronics of actuator 2 generates an electrical command to the clutch of actuator 1, thereby releasing the clutch and allowing the healthy actuator 2 to drive the flight control surface with minimum additional

drag torque developed by the failed actuator. This is possible for all failure cases except for a jam of the rollerscrew, which must be signaled in advance by the system health monitoring. A symmetrical behavior occurs if a failure originates in actuator 2. In the extremely unlikely event of a combination of failures leading to a total loss of the two actuators, no release signal is received from the two actuators clutches, which are thus in their engaged status allowing the flight control surface to backdrive the electric motors. While unpowered, the electric motors windings are connected to an internal circuitry in the motor drive electronics that dissipate energy, thereby providing an effective damping to the flight control surface. The electric motor is of a brushless dc type; the motor shaft is equipped with a resolver sensing the rotor position, hence allowing the motor drive electronics to perform the correct commutation of the electrical currents and the electronic control unit to receive position information and to compute the motor speed. The motor drive electronics (MDE) receives the speed commands from the electronic control unit (ECU), accepts the 115 V_{ac} power supply from the aircraft electrical system, converts it into a 270 V_{dc} voltage and generates the motor currents performing electric motor current control. The MDE also receives a discrete enable signal from the ECU, which allows the activation of the electrical power supply to the motor power bridge and an isolate signal from the ECU monitoring logic. The discrete enable signal is sourced by the ECU control section. It is a discrete signal that is opto-isolated in the MDE. It controls a power mosfet switch that switches on/off the supply voltage

Figure 4: Control system architecture

to the 3-phase power bridge. The absence of the signal disables the power drive. The enable circuit is also used to protect against overcurrent pulled by the power bridge. Thus in the case of such events as a short to chassis of a motor phase wire when unusual high currents are developed, the power switch in the MOSFET is quickly switched off, thus preventing consequential damage to other MDE components. A further function of the enabling circuit is to limit the inrush current to the power module bulk capacitors on the power bridge when the power module is initially enabled. The isolate signal is generated by the ECU monitoring section and operates in the same way of the enable signal through a circuitry that is completely independent of the enable signal circuitry. The MDE can dissipate the regeneration energy by means of a resistive dump when the flight control surface is operated in aiding load conditions and rapid motor braking conditions; no energy is then allowed to go back to the aircraft supply bus. The flight control surface position is measured by two LVDTs mounted on the two actuators. Each transducer is dual electrical, with its two sections interfacing with the control and monitoring sections of the ECU. The ECU is itself a unit comprised of two separate sections: control and monitor, each operating on a different microprocessor. The control section provides both the excitation and the demodulation of one section of the actuator position transducer, while the same is done with the other section of the position transducer by the ECU monitoring section. The two position signals obtained from the position transducer of one actuator are passed to the ECU of the other actuator via a cross channel data link (CCDL) and viceversa, so that each ECU has available four position signals and performs

their consolidation and monitoring. The ECU receives the position commands from the aircraft flight control computer and its control section performs the position control of the actuator using a regulation law optimized for achieving the best dynamic performance and dynamic stiffness. The ECU monitoring section implements a system health management as will be described later in this paper. System health status is sent to the aircraft central maintenance panel with a high recursion rate through a serial link. The ECU also includes an interface for connection to a ground unit, thereby allowing the possibility of uploading and downloading data and software.

5 CONTROL SYSTEM

The block diagram of Fig.4 describes the architecture of the control system. The ECU receives the position command from the FCCs, closes the actuator position and motor speed loops, and generates the current command to the motor drive electronics, while the MDE accepts the current command from the ECU and closes the current loop while modulating and phasing the supply voltage (and hence the currents) to the windings of the brushless motor. Position and speed are therefore digitally controlled, while the motor current is analogically controlled. The ECU uses both the signals provided by the actuators LVDTs and the position of the rotor of its own electric motor as information to close the position control loop. The LVDTs provide an absolute reference, while the rotor position provides an incremental signal. It was described in the previous section that each actuator is equipped with a dual electrical LVDT, so that

each actuator generates a dual redundant position signal. The two signals of each actuator are mutually exchanged between the two ECUs, so that each ECU has available four position signals that are used by the consolidation logic to generate the consolidated position signal and by the monitoring logic to perform monitoring and diagnosis of the system health. When ECU and MDE are switched on, the position feedback is set equal to the consolidated position and the signal obtained from the rotor position sensor is considered as the zero reference for the ensuing actuator operation. This initialization procedure performs a homing of the position feedback to the consolidated absolute position of the actuators. Starting from there, when the actuator moves, the position feedback for each actuator is obtained from the integration with time of the rotor position signal of the relevant electric motor. This provides a much greater position accuracy because of the very large kinematic ratio between motor angle and actuator linear output displacement. A concern about using the rotor position signal for position feedback is the possibility of losing the correct count of the number of revolution of the rotor. In order to counter this possible fault, a comparison between the consolidated position and the position indication obtained from the rotor signal integration is continuously performed. In case a discrepancy greater than a given threshold is recognized, then the rotor position information is discarded and the actuator position loop is performed simply setting the position feedback equal to the consolidated position. The position control law follows a non-linear PI scheme, where the contribute of the integrator path is saturated to a level such to allow to cancel the steady state errors under maximum load, while preventing unacceptable overshoots in case of large step commands; a small dead band is also applied on the integrator input, with the aim of preventing the insurgence of limit cycle oscillations that could result from an adverse combination of actuator backlash and friction with the integrator function. The output of the position control loop makes up the input to the internal speed control loop, whose functions are to improve the dynamic response and provide damping to the external position control loop. The control law implemented in the speed loop is a pure proportional gain since no stringent accuracy is needed for the actuator speed control. The control signal determined by the speed control loop is converted from digital to analogue and routed to the MDE that uses it as an input for the internal current control loop that eventually establishes the current of the electric motor. A critical issue with forced summed actuators is the possible occurrence of force fighting between the two actuators, in particular when the controlled aerodynamic surface is subjected to low external load, as it commonly happens during on-ground operations. In these condition, small differences in the physical characteristics of the MDEs and electric motors of the two actuators could lead to different motor output torques for the same current command received from the two MDEs. As a worst possible case, the aerodynamic surface would be kept stationary with the two actuators providing forces in opposite directions, which would cause surface twisting, unnecessary energy consumption and unwanted heating of the electric motors and the electronic drive. In order to mitigate the force fighting effects and possibly prevent its occurrence, the motor currents measured by the two MDEs are also routed to the two ECUs, where they are compared and an equalization signal is generated as indicated in the block diagram of Fig. 4. This signal is added or subtracted to the current command signal generated by the speed control loops of the two ECUs, which contributes to reducing the differences between the motors currents. The signals equalization logic is active only when both actuators are operating and is based on a dedicated PI law in which the integrator gain is varied with time when the equalization logic is activated, starting from an initial large value at switch-on to a smaller one after the initial equalization transient has settled. Both the maximum and the minimum value of the integrated signal are saturated a-priori. The output signals from the integrator and proportional gains are summed up and the resulting equalization signal is saturated to a maximum/minimum limit. Hence it is injected with the appropriate sign into the summing points of the forward paths of the two servoactuators control loops.

6 DESIGN CASE AND PERFORMANCE

The architecture outlined in the previous section was considered for the actuation system of the primary flight control surface of a large UAV with the following main characteristics:

- Flight control surface travel: ±30°
- Moment arm: 70 mm
- Maximum hinge moment (stall): 3500 Nm
- Design point (maximum power): 1200 Nm @ 55 °/s
- Maximum hinge moment induced by a gust: 300 Nm
- Maximum altitude: 13700 m (45000 ft)
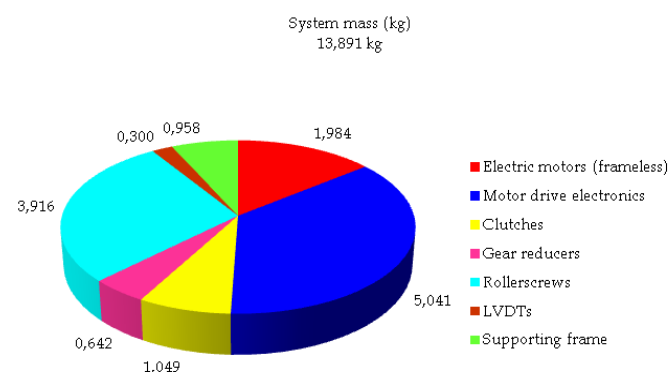- Electrical power supply: 270 V_{dc} nominal (variable from 235 to 285 V_{dc})

Figure 5: Actuator mass breakdown

An optimization design process was performed leading to the selection of a rollerscrew with 1.5 mm lead and a single stage gear reducer with 1/4.21 driven by a high-performance brushless dc motor. The electric motor has a torque sensitivity of 0.191 Nm/A, an electrical resistance of 2.64 Ω, an inductance of 0.98 mH, a thermal resistance of 1.8 °C/W, a viscous damping coefficient of 5.83×10^{-5} Nms/rad, a friction torque of 0.04 Nm, a cogging torque of 0.015 Nm and a moment of inertia of 3.1×10^{-5} kgm^2. The electric motor is a frameless unit with a mass of 0.992 kg accommodated inside the actuator housing in order to obtain a compact assembly. At the design point, the electric motor rotates at an angular speed of 12700 rpm. The ECU is a microprocessor-based controller closing the motor speed loop with a recursion rate of 4000 Hz and a computation time of 0.15 ms, while the position loop is operated at a recursion rate of 1000 Hz and a computation time of 0.6 ms. Analogue to digital conversion is performed with a 16-bit A/D converter. The overall mass of each actuator, inclusive of the control and power electronics (ECU + MDE) is 13.89 kg and, as described in Fig. 5, it can be split almost in half between the contribute of the electrical parts of the system (MDE, electric motor) and that of the mechanical components (transmission elements, sensors, supporting frame). The main system's performances have been evaluated through steady-state analysis in nominal and off-nominal conditions, as well as through dynamic simulations based on high-fidelity models built in Matlab\Simulink. The most important characteristics of the actuation system are summarized hereunder.

- Electrical power consumption at design point (nominal loading conditions, nominal efficiencies and nominal motors characteristics): 1183 W
- Maximum continuous load at zero speed for 70 °C ambient temperature: 1100 Nm
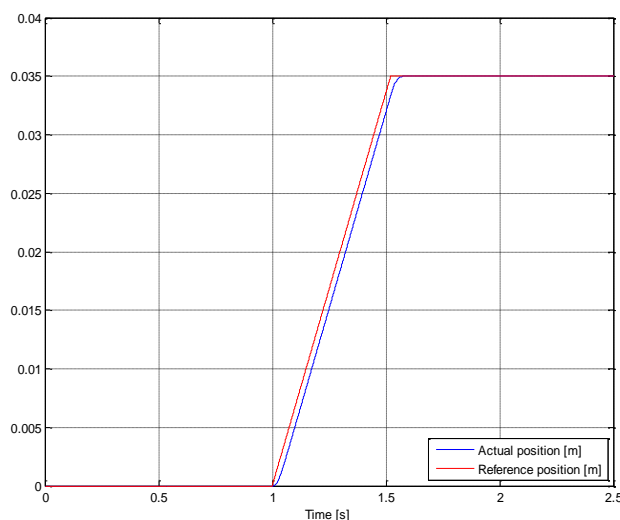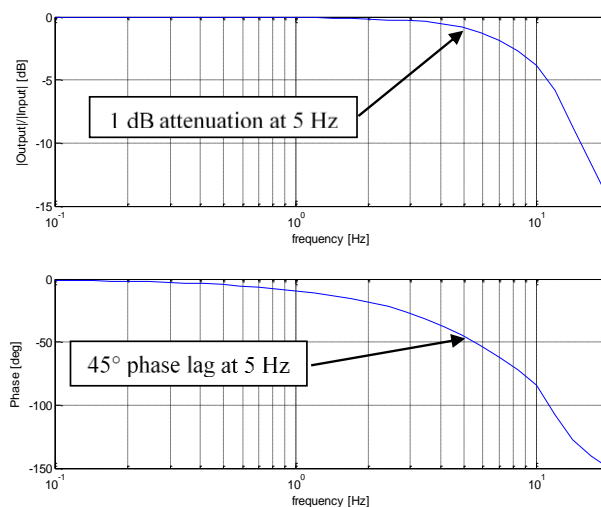

Figure 6: System response to a ramp command

Figure 7: System frequency response

- Stability margins for the position loop: 60° phase margin / 14.5 dB gain margin, which are well in-line with the usual requirements for primary flight control systems
- Response to a ramp command with the maximum rate of 55 °/s, corresponding to 67.2 mm/s of actuator linear speed: the maximum position error during actuation is 1.7 mm corresponding to 2.4% of full travel. Results are shown in Fig. 6.
- Frequency response: 45° phase lag at 5 Hz, 3 dB attenuation at 8.8 Hz under nominal loading conditions. The response is reported in Fig. 7.

7 HEALTH MANAGEMENT SYSTEM

The Health Management System is comprised of several functions that can be grouped into two main categories:

- Actuator failures monitor
- Prognostics and Health Management (PHM)

The failures monitor routines works to detect and classify potentially critical failures possibly occurring during flight and to highlight the presence of dormant failures through short pre-flight checks. Through continuous monitoring of the available information, the system is able to detect the following failure modes:

- Failure of one or more position sensors, which is detected by checking the summed output voltage of each LVDT section and by comparing the signals of the LVDTs
- Loss of coherence between the rotor position signal and the actuator LVDTs signals
- Uncontrolled electrical currents
- Actuator stall
- Uncommanded movement of the actuator
- Excessive twist of the flight control surface

- Overheating of the electric motor windings and of the MDE power bridge
- Failure of the ECU, which is detected by the ECU self-monitoring (check sum, watchdog, wraparound of output on input, permanent exchange of information between ECU control and monitoring sections via digital bus, with consolidation and validation, and permanent monitoring)

Pre-flight checks are performed before flight initiation to address the availability of the actuators components and to detect the presence of dormant failures, such as the inability of a clutch to release during flight. The prefight checks include:

- ECU built-in-test at power-up
- Check of the clutches operation. Electrical commands are given to release the clutches, while at the same time a position command is given. If an actuator movement is recorded, that implies a failure of the clutch to open. Then, no release signal is sent to the clutches and the actuators are in turn commanded to move. Lack of actuator output movement indicates a failure of the clutch to engage.

The Prognostic and Health Management system is designed to detect and properly classify a pre-defined number of anticipated faults, to track their and predict their evolution while providing convergent estimates of the actuator's Remaining Useful Life (RUL). This system works on slowly evolving degradations, i.e. requiring more than a few flights to reach a critical size, and its primary objectives are to enhance the vehicle availability, reduce unexpected on-ground downtime and provide means to allow for better maintenance and mission planning. The presence of the continuous failure monitoring is thus still required to properly manage the occurrence of sudden failures, providing an additional layer of information on the system health status. The PHM system operates on data acquired both in-flight and during dedicated pre-flight tests designed to highlight the effects of faults which may be difficult to detect during the missions, such as the backlash growth in the actuator-surface joints. The dedicated pre-flight tests are performed over the following short procedure. Actuator 1 is at first commanded with four periods of a 2 Hz sinusoid, featuring zero mean and amplitude of 5% of the actuator stroke. Hence a full stroke is performed at a constant speed equal to 50% of the rated speed. The test is repeated over the following conditions:

- Clutch of actuator 1 released (sinusoid only)
- Clutch of actuator 1 engaged, clutch of actuator 2 released (sinusoid only)
- Clutch of actuator 1 engaged, clutch of actuator 2 engaged, electric motor of actuator 2 unpowered

The same sequence of operational tests is then repeated by commanding actuator 2, resulting in an overall duration
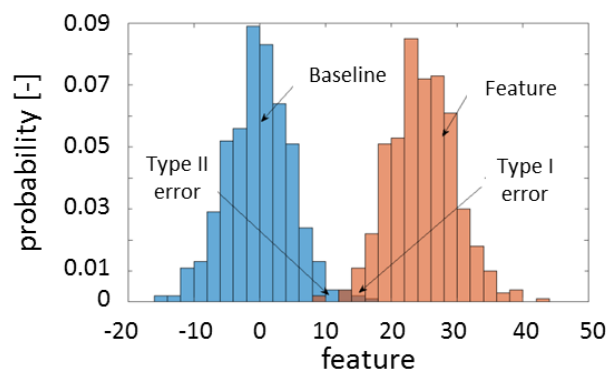

Figure 8: Type I and Type II errors

of 12 s. The main objective of this test sequence is to stress the actuators in both steady-state (constant speed commands) and dynamic conditions (sinusoid, motion inversion); moreover, this approach allows to separately study each major component of the mechanical transmission by exploiting each of the possible combination for the clutch engagement. During pre-flight tests and during flight, the system acquires the available signal coming from the actuator, such as position commands, phase currents and supply tensions of the electric motors, rotor position and LVDTs measures. Other information, whereas available in the UAV's systems, are collected as well, such as the external temperature, the vehicle attitudes, the dynamic pressure field beneath the wing. Each signal is at first validated and hence sent to the PHM module. The PHM module operates through four different layers:

- Signal conditioning/feature or condition index extraction
- Anomaly/fault detection
- Fault isolation/identification
- Failure prognosis/RUL estimate

The first layer is dedicated to extract from the available raw data a certain number of pre-defined indexes representative of the actuators health status. We distinguish in this case between features and condition indexes. A Condition Index (CI) is an index such that is sensitive to changes in the health status of the monitored system, while a feature is a quantity, possibly a combination of several CIs, which behaviour is highly correlated with that of the associated degradation and ideally uncorrelated with that of any other fault [26]. The second layer performs the anomaly/fault detection through a purely data-driven algorithm. Data distributions for each feature and each CI are continuously computed and compared with their baselines defined for healthy conditions. For each baseline, a threshold is defined in correspondence of a pre-defined percentile (usually the 95th). The fault is declared when a predefined percentage of the feature distribution (usually 95%) overcomes said threshold, generating an alarm signal. This approach has the benefits of being system-agnostic, since there is no need of fine-tuning the threshold, while

allowing for the a-priori definition of the Type-I and Type-II errors (false positive and false negative), as in Fig. 8[26]. Whenever an alarm signal is generated, the alarm vector, containing the values of the alarm flags for each monitored index, and the feature vector are sent as input to the third layer. This level performs the fault isolation and identification, which means to assess the type of the occurring faults, their location and its or their severity. This task is performed through a properly trained Artificial Neural Network (ANN), which provides an alarm code to the next layer and to the aircraft Health Usage and Monitoring System (HUMS). The final layer of the PHM module receives the feature vector and the alarm codes, making use of an enhanced Particle Filter framework to track the faults growth and estimate the RUL starting from off-line defined degradation models [27]. The Particle Filter makes use of an off-line defined, non-linear degradation model, a tunable non-linear evolution model and non-Gaussian description of measuring and process noises to estimate the fault size and project their evolution in time. The system is designed to recognize the following failure modes.

- Backlash increase in the spherical joints connecting the screws with the control surface, through comparison of the position signals coming from the LVDTs of the two actuators

- Rollerscrew and gear reducer backlash increase resulting from the components wear, through comparison of the position signals coming from the resolver on the motor shaft and the LVDT of the linear actuator

- Increase of friction of the actuator mechanical components potentially leading to a seizure, through efficiency analysis during dedicated pre-flight checks

- Reduction of the torque transmission capability of the clutches, or failures of the clutches to open, through study of the movements performed during pre-flight checks.

- Degradation of the motor's permanent magnets, through efficiency analysis performed during flight and confirmed on-ground during pre-flight checks

- Short circuit occurrence in the motor windings due to ageing of the insulating materials, through detection of asymmetries in the current's profiles [28]

- Anomalies or failures of the motor drive electronics, such as base drive open circuit conditions, short circuit in the DC-Link, capacitors degradations etc. [29]

It is important to highlight that not every degradation can be recognized through the analysis of in-flight data. As an example, the total backlash on each actuator, as well as its repartition between each component, can be studied only through pre-flight data. In practice, every degradation that can be expected in service can be recognized at different stages of its development by one of the components of the Health Management System, that is either the PHM module (early fault detection and prognosis) or the failures monitor through C-Bit and P-Bit. The general architecture of the health management system is shown in the block diagram of Fig. 9. If any fault or failure is recognized, an alarm is raised and the information sent to the aircraft Health Usage and Monitoring System (HUMS), along with the RUL estimate, if available. If a faulty condition is detected, the HUMS can hence make use of these information to reconfigure the actuators control in the attempt to slow
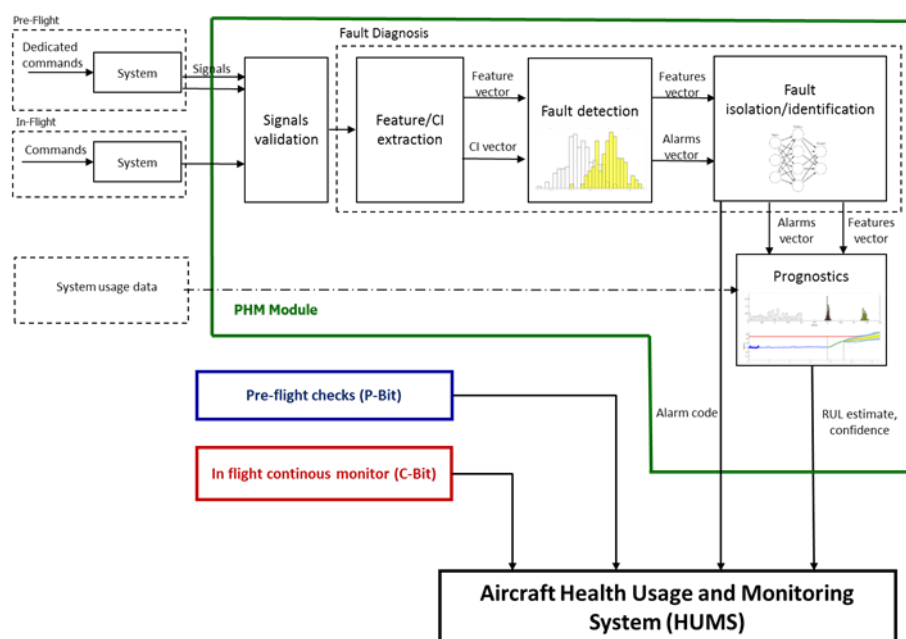

Figure 9: General architecture of the system health management

down the degradation growth, and/or mitigate the performance drops associated with the anomalous behaviour [30].

8 PHM CASE STUDY AND PERFORMANCEHEALTH MANAGEMENT SYSTEM

To better describe the PHM module behavior we resort to a single-fault scenario case study; data for this study have been obtained by corrupting the parameters of the actuators high-fidelity dynamic model through degradation laws available in literature. As such, the following considerations were employed

- Wear progression in mechanical components (clutches, gearbox, screw and rod-end) has been described through Archard's model given an estimated usage pattern and modeled as elasto-backlash of increasing size [31]

- The degradation of the insulating material of the electric motor has been modelled following the Arrhenius law according to the approach presented in [30].

- Degradation of the permanent magnets of the brushless motor has been approximated by combining the simulated temperature of the windings with the demagnetization model proposed in [32].

- Degradations in the motor drive electronics have been modeled as fast-occurring failures.

The anomaly detection algorithm is able to successfully recognize the inception of the selected faults, providing early alerts in correspondence of an average size of the defect equal lower than 20% of their critical value. The inception of turn-to-turn shorts in the motor windings is detected within the 11.75% of its progression, the magnets degradation within 12.3%, while the wear in the mechanical transmission and in the rod-end is detected respectively within the 8.5% and the 22% of the critical value, assumed to be equal to 0.2 times the screw pitch. These mean values can vary depending on the application, fault evolution patterns and on the accuracy of the employed sensors. An example of the output of the fault detection algorithm is reported in Fig. 10, where the system detects the presence of wear in the mechanical transmission (MT − WEAR) and the insurgence of magnets degradation in the electric motor (EM − DMD): a label is assigned to each feature used to monitor the evolution of the associated fault. Both the baseline values (in white) and the current values of the features are reported (in red, if faulty, in yellow if healthy), as well as the alarm flags and the associated confidence. Once that the fault has been detected and successfully classified, the prognostic routines are called to predict the faults evolution and the associated RUL. An example of the output of the Particle Filter framework for the degradation of the magnets in the electric motor is reported in Figs. 11, where we can observe the probability distributions associated with the feature values and the estimated fault size (hidden state) in correspondence of the fault detection and of the prediction instant. For each prediction, three values of RUL are defined, each associated with a prediction confidence of 5%, 50% and 95%. We address
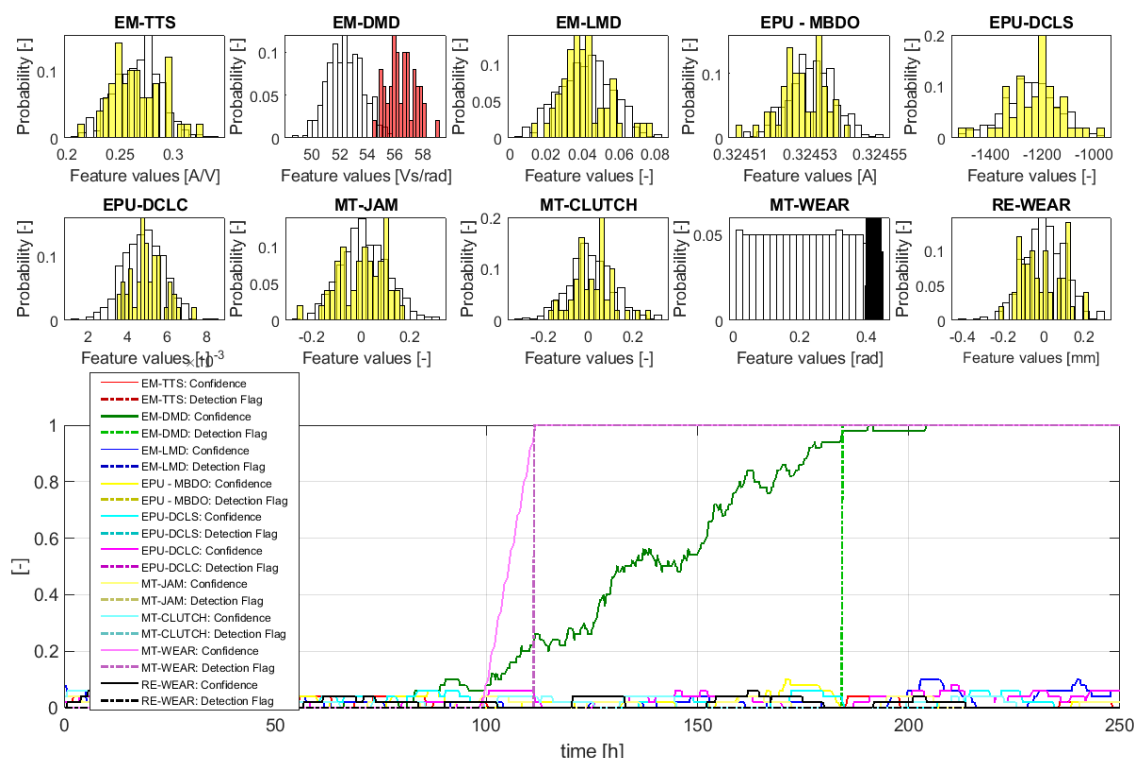

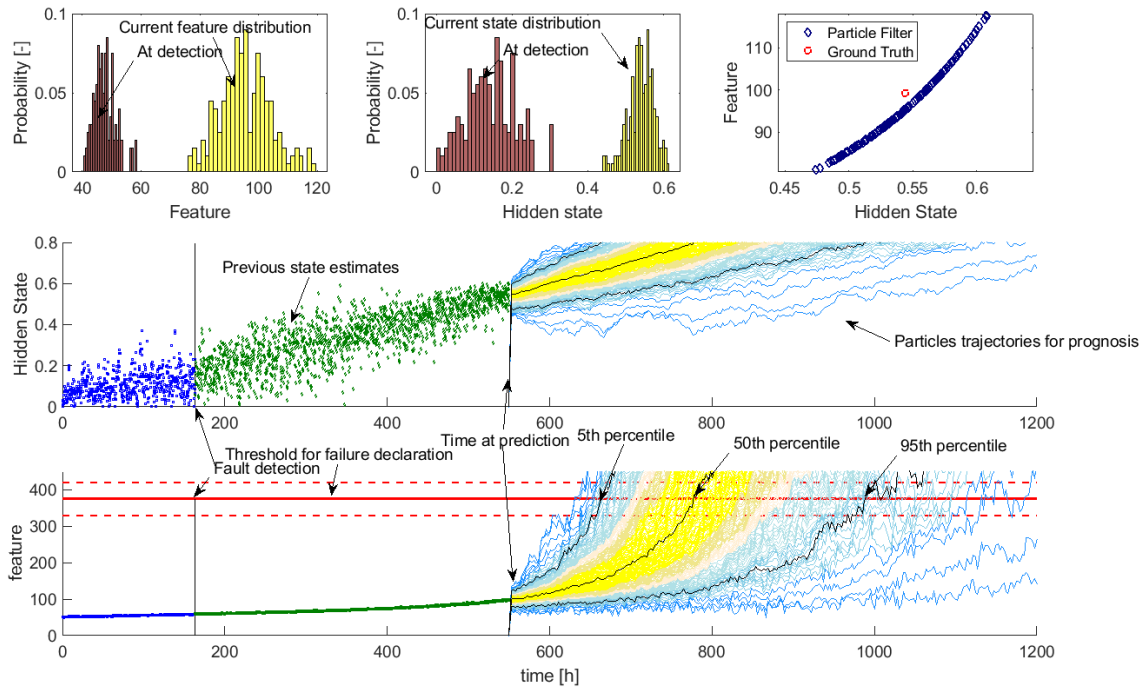Figure 10: Example of fault detection

Figure 11: Prognostic framework - example

each of these values as "early maintenance RUL", "advised maintenance RUL" and "late maintenance RUL". These three values tend naturally to convergence toward the latest stages of the fault evolution. Typically, the RUL estimate associated with the 50% confidence is the one used as reference. To each anomalous condition corresponds a different Particle Filter call and hence a different RUL estimate. In the unlikely case of multiple faults occurrence, the PHM module will output as RUL of the system the minimum between the estimated RULs computed for each detected anomalous condition. To assess the performance of the prognostic framework we resort to the state-of-the-art metrics defined by Saxena and others in [33], in particular the $\alpha-\lambda$ analysis, which leads to the definition of the prognostic horizon (PH), the Relative Accuracy (RA) and the Cumulative Relative Accuracy (CRA). The $\alpha-\lambda$ analysis, better explained through Fig. 12, is a graphical tool used to represent the RUL vs time behaviour in non-dimensional form; on the abscissa, time is reported as

$$\lambda = \frac{t - t_{det}}{t_{EOL} - t_{det}} \tag{1}$$

Where t_{det} it the time at fault detection, t_{EOL} is the time at End of Life of the component and t is the time at prediction. Its value can range between 0 and 1. On the ordinate, the RUL is reported as the ratio between the predicted RUL and the real one. The "ground truth" is represented by a straight line along with a tolerance band on the prediction, usually defined as ±20%. The Prognostic Horizon (PH) is defined as the real RUL for witch the prediction first falls inside the

tolerance band and is an expression of the time interval in which the prognostic output can be trusted. The Relative Accuracy is defined as,

$$RA = 1 - \frac{|RUL_r - RUL|}{RUL_r} \tag{2}$$

Where RUL_r is the real RUL. Its cumulative value (CRA), is used to assess the convergence of the RUL estimate by weighting the RA values as,

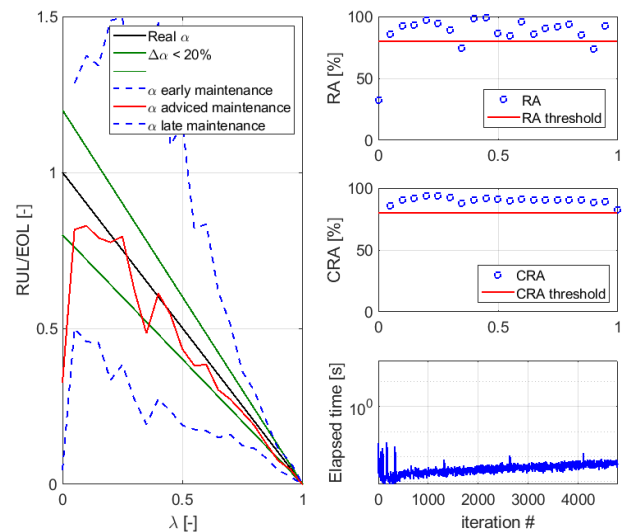$$CRA = \frac{1}{\sum_i \lambda_i} \sum_i \lambda_i RA_i \tag{3}$$

Figure 12: Prognostic performance for magnets degradation

For the degradations of this case study, the prognostic framework performs well, providing prognostic horizons of 64 flight hours (FH) for the turn-to-turn short in the motor windings (87.91% mean RA, 93.1% CRA), 82 FH for the magnets degradation (83.6% mean RA, 82.4% CRA), 130 FH for the wear in the mechanical transmission (80.1% mean RA, 80.4% CRA) and more than 300 FH for the wear in the rod-end (82.1% mean RA, 81.6% CRA). The algorithm has been tested on an *Intel-7@2.60GHz* and has proven to be suitable for on-line operations, with each iteration lasting less than 0.01 s.

9 CONCLUSIONS AND FUTURE WORK

The architecture and the performance of the robust architecture for EMA flight controls have been presented and discussed, detailing the design issues and their possible solutions while providing additional information through a dedicated case study. The structure and the performance of the health management system of the mechatronic device have been presented as well; the presented architecture, based on the synergy between the traditional built-in-tests (C-Bit and P-Bit) and novel prognostics techniques combining in-flight data with dedicated pre-flight checks, has shown promising results that would allow for increased safety and availability of electromechanical actuators for primary flight control surfaces. Further work is under way to perform a feasibility study on the application of the presented prognostic techniques to single points of failures that can lead to the actuator jamming. The consequent definition of a comprehensive health management system would allow to tackle new actuation technologies and flight control architectures, promoting the use of novel design methodologies to consider PHM system since the first stages of the project.

NOMENCLATURE

λ Adimensional time for PHM analysis

CRA Cumulative Relative Accuracy

RA Relative Accuracy

RUL Remaining Useful Life

RUL_r Real Remaining Useful Life

t Time

t_{EOL} Time of Failure

t_{det} Time at Fault Detection

REFERENCES

[1] Nelson J.D., Scalon J.F., *Ballistic Tolerant Dual Load Path Ballscrew and Ballscrew Actuator*, US Patent Number 4,679,485, July 14, 1987

[2] Hicks D., Operation and Redundancy of the V-22 Pylon Conversion Actuator, Presented at the *SAE A6 Committee, Aerospace Fluid Power and Actuation Systems*, Lake Tahoe, October 1992

[3] Kopala D.J., Doell C., High Performance Electromechanical Actuation for Primary Flight Surfaces, *Recent Advances in Aerospace Actuation Systems and Components 2001*, p. 135-139, June 13-15, 2001, Toulouse, France

[4] Office of the Secretary of Defense, *Unmanned Aerial Vehicles Roadmap* 2000-2025, April 2001

[5] Sandler S., Hervieux A., Electrical Flight Control Technologies for Rotorcrafts, *Recent Advances in Aerospace Actuation Systems and Components 2007*, p. 9-14, June 13-15, 2007, Toulouse, France

[6] Kulshreshtha A., Remote Actuation Control System: Aircraft Flight Control for Hydraulic-Servo & Electric Actuation, *Recent Advances in Aerospace Actuation Systems and Components 2007*, p. 155-162, June 13-15, 2007, Toulouse, France

[7] Gerada C., Bradley K., Whitley C., Towers G., A Directly Driven EMA for Aerospace Applications, *Recent Advances in Aerospace Actuation Systems and Components 2007*, p. 81-86, June 13-15, 2007, Toulouse, France

[8] Wheeler P., Whitley C., Towers G., Design and Reliability of a Rudder EMA with an Integrated Permanent Magnet Machine and Matrix Converter Drive, *Recent Advances in Aerospace Actuation Systems and Components 2007*, p. 93-98, June 13-15, 2007, Toulouse, France

[9] Wachendorf N., Carl U.B., Thielecke F., Control and Monitoring of a Trimmable Horizontal Stabilizer Actuator with Two Primary Load Paths, *Recent Advances in Aerospace Actuation Systems and Components 2007*, p. 105-110, June 13-15, 2007, Toulouse, France

[10] Shäfer I., Kayser A., Smart Electromechanical Utility Actuator, *Recent Advances in Aerospace Actuation Systems and Components 2007*, p. 177-182, June 13-15, 2007, Toulouse, France

[11] Whitley C., Roper J., Development, Manufacture & Flight Test of Spoiler EMA System, *Recent Advances in Aerospace Actuation Systems and Components 2007*, p. 215-220, June 13-15, 2007, Toulouse, France

[12] Facey W., Overview of the MQ-8B Fire Scout VTUAV, Presented at the *SAE A6 Committee, Aerospace Fluid Power and Actuation Systems*, Daytona Beach, April 20-24, 2008

[13] Lucas W., Seward M., Electro-Mechanical Actuation in Unmanned Aerial Vehicle Applications, Presented

at *the SAE A6 Committee, Aerospace Fluid Power and Actuation Systems*, Daytona Beach, April 20-24, 2008

[14] Decker W., Perrin U., Flight Control Actuation System of an UAV, Presented at the *SAE A6 Committee, Aerospace Fluid Power and Actuation Systems, Daytona Beach*, April 20-24, 2008

[15] Polcuch E., State-o-the-Art in UAV Actuation, Presented at the *SAE A6 Committee, Aerospace Fluid Power and Actuation Systems*, Daytona Beach, April 20-24, 2008

[16] Recksiek M., Advanced High Lift System Architecture with Distributed Electrical Flap Actuation, *Proceedings of the 2ⁿᵈ International Workshop on Aircraft System Technologies*, March 26 – 27, 2009, Hamburg, Germany

[17] Todeschi M., Airbus - EMAs for Flight Controls Actuation Systems - Perspectives, *Recent Advances in Aerospace Actuation Systems and Components 2010*, p. 1-8, May 5-7, 2010, Toulouse, France

[18] Christmann M., Seemann S., Jäker P., Innovative Approaches to Electromechanical Flight Control Actuators and Systems, *Recent Advances in Aerospace Actuation Systems and Components 2010*, p. 17-23, May 5-7, 2010, Toulouse, France

[19] Babinski J.A., Jam Tolerant Electro-Mechanical Actuators for Aircraft Flight and Utility Control, *Recent Advances in Aerospace Actuation Systems and Components 2010*, p. 42-46, May 5-7, 2010, Toulouse, France

[20] Curran S., Walters T.E., Chirico A.J., Health Monitoring and Prognostics for Electromechanical Actuation, *Recent Advances in Aerospace Actuation Systems and Components 2010*, p. 47-55, May 5-7, 2010, Toulouse, France

[21] De La Chevasnerie A., Grand S., Legrand B., Sandler S., Electromechanical Actuator / Moet Project, *Recent Advances in Aerospace Actuation Systems and Components 2010*, p. 83-87, May 5-7, 2010, Toulouse, France

[22] Alexandre P., Telteu D., Baudart F., Labrique F., Matagne E., Failure Operation of a Multiphase Drive for an Electromechanical Actuator, *Recent Advances in Aerospace Actuation Systems and Components 2010*, p. 111-115, May 5-7, 2010, Toulouse, France

[23] Isturiz A., Vinals J., Fernandez S., Basagotti R., De La Torre E., Novo J., Development of an Aeronautical Micro Electromechanical Actuator with Real Time Health Monitoring Capability, *Recent Advances in Aerospace Actuation Systems and Components 2010*, p. 145-153, May 5-7, 2010, Toulouse, France

[24] Nierlich F., Anee E., Farid A., Liegeois P-Y., Leynaert F-N., More Electrical Actuation: Modular Power Electronics & Electrical Motors Concepts, *Recent Advances in Aerospace Actuation Systems and Components 2010*, p. 154-159, May 5-7, 2010, Toulouse, France

[25] Keech N.K., Cyrot, L.P., Polcuch E.A., *Aircraft Stabilizer Actuator*, US Patent Application Publication Number US 2011/0048147 A1, March 3, 2011

[26] Vachtsevanos, G., Lewis, F. L., Roemer, M., Hess, A., & Wu, B. (2006). *Intelligent fault diagnosis and prognosis for engineering system*. Hoboken, NJ: John Wiley & Sons, Inc.

[27] Orchard M. (2007). *A particle filtering-based framework for on-line fault diagnosis and failure prognosis*. Doctoral dissertation, Georgia Institute of Technology, Atlanta, GA, USA.

[28] De Martin A., Jacazio G., Vachtsevanos G., Windings Fault Detection and Prognosis in Electro-Mechanical Flight Control Actuators Operating in Active-Active Configuration, *International Journal of Prognostics and Health Management* 8, 2017.

[29] Brown B., Abbas M., Ginart A., Ali I., Kalgren P., Vachtsevanos G. (2010). Turn-off time as a precursor for gate bipolar transistor latch-up faults in electric motor drives. *Annual conference of the Prognostics and Health Management Society*, October 10ᵗʰ-16ᵗʰ, Portland, OR, USA.

[30] Brown B., Geogroulas G., Bole B., Pei H.L., Orchard M., Tang L., Saha B., Saxena A., Goebel K., Vachtsevanos G. (2009). Prognostics enhanced reconfigurable control of electro-mechanical actuators. *Annual conference of the Prognostics and Health Management Society*, September 27ᵗʰ-October 1ᵗʰ, San Diego, CAL, USA.

[31] Nordin M., Gallic J., Gutman P.O. (1997), New models for backlash and gear play. *International Journal of Adaptive Control and Signal Processing* 11, pp.49-63.

[32] Ruoho S., Dlala E., and Arkkio A. (2007). Comparison of Demagnetization Models for FiniteElement Analysis of Permanent-Magnet Synchronous Machines. *IEEE Trans. Magn.* 43, pp. 3964-3968.

[33] Saxena A., Celaya J., Balaban E., Goebel K., Sasha B., Schwabacher M. (2008). Metrics for evaluating performance of prognostic techniques, *International Conference on Prognostics and Health Management*, October 6ᵗʰ-9ᵗʰ, Denver, CO, USA.

TEMPLATE FOR PREPARING PAPERS FOR PUBLISHING IN INTERNATIONAL JOURNAL OF MECHANICS AND CONTROL

Author1*   Author2**

* affiliation Author1

** affiliation Author2

ABSTRACT

This is a brief guide to prepare papers in a better style for publishing in International Journal of Mechanics and Control (JoMaC). It gives details of the preferred style in a template format to ease paper presentation. The abstract must be able to indicate the principal authors' contribution to the argument containing the chosen method and the obtained results. (max 200 words)

Keywords: keywords list (max 5 words)

1 TITLE OF SECTION (E.G. INTRODUCTION)

This sample article is to show you how to prepare papers in a standard style for publishing in International Journal of Mechanics and Control.

It offers you a template for paper layout, and describes points you should notice before you submit your papers.

2 PREPARATION OF PAPERS

2.1 SUBMISSION OF PAPERS

The papers should be submitted in the form of an electronic document, either in Microsoft Word format (Word'97 version or earlier).

In addition to the electronic version a hardcopy of the complete paper including diagrams with annotations must be supplied. The final format of the papers will be A4 page size with a two column layout. The text will be Times New Roman font size 10.

Contact author: author1[1], author2[2]

[1]Address of author1.

[2]Address of author2 if different from author1's address
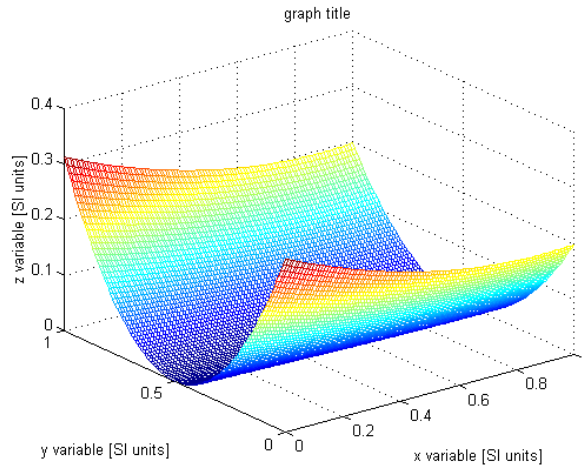E-mail: author1@univ1.com , author2@univ2.com

2.2 DETAILS OF PAPER LAYOUT

2.2.1 Style of Writing
The language is English and with UK/European spelling. The papers should be written in the third person. Related work conducted elsewhere may be criticised but not the individuals conducting the work. The paper should be comprehensible both to specialists in the appropriate field and to those with a general understanding of the subject.

Company names or advertising, direct or indirect, is not permitted and product names will only be included at the discretion of the editor. Abbreviations should be spelt out in full the first time they appear and their abbreviated form included in brackets immediately after. Words used in a special context should appear in inverted single quotation mark the first time they appear. Papers are accepted also on the basis that they may be edited for style and language.

2.2.2 Paper length
Paper length is free, but should normally not exceed 10000 words and twenty illustrations.

2.2.3 Diagrams and figures
Figures and Tables will either be entered in one column or two columns and should be 80 mm or 160 mm wide respectively. A minimum line width of 1 point is required at actual size. Captions and annotations should be in 10 point with the first letter only capitalised *at actual size* (see Figure 1 and Table VII).

Figure 1 Simple chart.

Table VII - Experimental values

Robot Arm Velocity (rad/s)	Motor Torque (Nm)
0.123	10.123
1.456	20.234
2.789	30.345
3.012	40.456

2.2.4   Photographs and illustrations

Authors could wish to publish in full colour photographs and illustrations. Photographs and illustrations should be included in the electronic document and a copy of their original sent. Illustrations in full colour …

2.2.5   Equations

Each equation should occur on a new line with uniform spacing from adjacent text as indicated in this template. The equations, where they are referred to in the text, should be numbered sequentially and their identifier enclosed in parenthesis, right justified. The symbols, where referred to in the text, should be italicised.

- point 1
  - point 2
    - point 3
1. numbered point 1
   2. numbered point 2
      3. numbered point 3

$$W(d) = G(A_0, \sigma, d) = \frac{1}{T} \int_0^{+\infty} A_0 \cdot e^{-\frac{d^2}{2\sigma^2}} dt \qquad (1)$$

3   COPYRIGHT

Authors will be asked to sign a copyright transfer form prior to JoMaC publishing of their paper. Reproduction of any part of the publication is not allowed elsewhere without permission from JoMaC whose prior publication must be cited. The understanding is that they have been neither previously published nor submitted concurrently to any other publisher.

4   PEER REVIEW

Papers for publication in JoMaC will first undergo review by anonymous, impartial specialists in the appropriate field. Based on the comments of the referees the Editor will decide on acceptance, revision or rejection. The authors will be provided with copies of the reviewers' remarks to aid in revision and improvement where appropriate.

REFERENCES (DESCRIPTION)

The papers in the reference list must be cited in the text. In the text the citation should appear in square brackets [ ], as in, for example, "the red fox has been shown to jump the black cat [3] but not when...". In the Reference list the font should be Times New Roman with 10 point size. Author's first names should be terminated by a 'full stop'. The reference number should be enclosed in brackets.

The book titles should be in *italics*, followed by a 'full stop'. Proceedings or journal titles should be in *italics*. For instance:

REFERENCES (EXAMPLE)

[1] Smith J., Jones A.B. and Brown J., *The title of the book*. 1st edition, Publisher, 2001.

[2] Smith J., Jones A.B. and Brown J., The title of the paper. *Proc. of Conference Name*, where it took place, Vol. 1, paper number, pp. 1-11, 2001.

[3] Smith J., Jones A.B. and Brown J., The title of the paper. *Journal Name*, Vol. 1, No. 1, pp. 1-11, 2001.

[4] Smith J., Jones A.B. and Brown J., *Patent title*, U.S. Patent number, 2001.

NOTE: Authors/copyright holders are asked to complete this form signing section A, B or C and mail it to the editor office with the manuscript or as soon afterwards as possible.	*Editorial Secretary address:* Andrea Manuello Bertetto Matteo D. L. Dalla Vedova, Lorenzo Pace *Dept. of Mechanical and Aerospace Engineering* *Politecnico di Torino* *C.so Duca degli Abruzzi, 24 – 10129 Torino – Italy* *e_mail: jomac@polito.it* *fax n.: +39.011.564.6999*

The article title:

_____

By:_____

To be Published in ***International Journal of Mechanics and Control JoMaC***
Official legal Turin court registration Number 5320 (5 May 2000) - reg. Tribunale di Torino N. 5390 del 5 maggio 2000

A   Copyright to the above article is hereby transferred to the JoMaC, effective upon acceptance for publication. However the following rights are reserved by the author(s)/copyright holder(s):
    1. All proprietary rights other than copyright, such as patent rights;
    2. The right to use, free or charge, all or part of this article in future works of their own, such as books and lectures;
    3. The right to reproduce the article for their own purposes provided the copies are not offered for sale.
       To be signed below by all authors or, if signed by only one author on behalf of all co-authors, the statement A2 below must be signed.

A1. All authors:

SIGNATURE_____DATE_____   SIGNATURE_____DATE_____

PRINTED NAME_____   PRINTED NAME_____

SIGNATURE_____DATE_____   SIGNATURE_____DATE_____

PRINTED NAME_____   PRINTED NAME_____

A2. One author on behalf of all co-authors:
"I represent and warrant that I am authorised to execute this transfer of copyright on behalf of all the authors of the article referred to above"

PRINTED NAME_____

SIGNATURE_____ TITLE_____ DATE_____

B. The above article was written as part of duties as an employee or otherwise as a work made for hire. As an authorised representative of the employer or other proprietor. I hereby transfer copyright to the above article to *International Journal of Mechanics and Control* effective upon publication. However, the following rights are reserved:
1.   All proprietary rights other than copyright, such as patent rights;
2.   The right to use, free or charge, all or part of this article in future works of their own, such as books and lectures;
3.   The right to reproduce the article for their own purposes provided the copies are not offered for sale.

PRINTED NAME_____

SIGNATURE_____ TITLE_____ DATE_____

C. I certify that the above article has been written in the course of employment by the United States Government so that no copyright exists, or by the United Kingdom Government (Crown Copyright), thus there is no transfer of copyright.

PRINTED NAME_____

SIGNATURE_____ TITLE_____ DATE_____

CONTENTS – Special Issue for IFIT 2018

CONTENTS – Regular Issue

Next issue titles will be from the selected and awarded papers of:

RAAD 2019

28th International Conference on Robotics in Alpe-Adria-Danube Region

Kaiserslautern, Germany
June 19-21, 2019